Eur. Phys. J. Appl. Phys. (2016) 74: 24614
DOI: 10.1051/epjap/2016150424

THE EUROPEAN PHYSICAL JOURNAL APPLIED PHYSICS

Regular Article

Solid-state structures and properties of scandium hydride; hydrogen storage and switchable mirrors application*

Khadidja Khodja[a], Youcef Bouhadda, Larbi Seddik, and Kamel Benyelloul

Unité de Recherche Appliquée en Energies Renouvelables, URAER, Centre de Développement des Énergies Renouvelables, CDER, 47133 Ghardaïa, Algeria

Received: 15 August 2015 / Received in final form: 17 February 2016 / Accepted: 19 February 2016
Published online: 3 May 2016 –

Abstract. First-principles calculation has been performed on the rare earth hydride ScH_2 for hydrogen storage and switchable mirror applications, using the pseudo-potentials and plane waves based on the density-functional theory (DFT). The electronic and structural properties are studied within both local-density and generalized gradient approximations for exchange energy. The formation energy and the optical properties have been investigated and discussed. Our calculated results are generally in good agreement with theoretical and experimental data.

1 Introduction

The combustion of hydrogen is non-polluting and highly energetic. Its use as a fuel in the near future is considered. Two major problems remain to be overcome to produce hydrogen gas in sufficient quantities: polluting synthesis methods (hydrocarbon cracking) and too low yield (water electrolysis). The hydrogen can be a dangerous gas because it is explosive in presence of air. However, its storage in the form of metal hydride (solid-state storage) provides a solution to this problem. Additionally, in this form it has a large volume storage capacity.

ScH_2 compound is a rare-earth metal-hydride used in switchable mirrors [1] and hydrogen storage [2,3]. Scandium is highly capable of accommodating hydrogen, either in its elemental state by the formation of ScH_2 [4,5], or as a component in intermetallic compounds such as $ScFe_2$ ($ScFe_2H_2$) and Sc_2Ni (Sc_2NiH_5) [6–8].

A good comprehension of the fundamental interactions between Sc atoms and hydrogen in ScH_2 and its properties, can be useful to improve some potential hydrides for hydrogen storage or switchable mirrors applications. Indeed, for hydrogen storage: Luo et al. [9] investigated the catalytic effect and the influence of ball milling duration of ScH_2, on the dehydrogenation of MgH_2. Also, Notten et al. [10] discovered a very large (reversible) storage capacity of 5.6 wt.% in $Mg_{0.8}Sc_{0.2}Pd_{0.024}$ (in a 6-M-KOH electrolyte at 25 °C) which is about four times more than in Ni-MH batteries.

For switchable mirrors applications, Weaver et al. [11,12] measured in detail the reflectivity of dihydrides of Sc, Y and La but they don't extend their interesting measurements to the trihydrides of Sc, Y and La. Griessen et al. [13] observed that Y-, La- and rare earth-hydride films exhibit optical switching near their metal-insulator transition: the dihydrides are metallic and shiny while the trihydrides are semiconducting and transparent. However, ScH_3 cannot be formed at atmospheric pressure, from pure Sc (only at 300 MPa hcp ScH_3 is formed [14]). But, Griessen et al. [1] confirmed the formation of ScH_3 in thin-films of Mg-Sc. These films become very transparent when the Mg content is larger than 65 at.%. Also, Messina et al. [15] studied the effect of systematic substitution of Sc for Y on the optical metal-to-insulator transition (MIT) in the $Y(1-x)Sc(x)$-hydrogen alloy system. They observed that the optical transmittance decreases significantly for $x > 0.10$ and confirm the transition from trihydride to dihydride behavior with increasing x.

The scandium hydride, ScH_2, of f.c.c. structure with a hydrogen content of 4.25 wt.% had been obtained by Dolukhanyan et al. [4,5].

The aim of this paper is to contribute to the investigation of electronic properties and heat of formation of ScH_2 using DFT based on pseudo-potentials and plane waves.

2 Computational details

Solid-state electronic structure calculations were carried out within density functional theory (DFT) [16]. We used both local-density approximation (LDA) of Troullier and

[a] e-mail: khodja_kh@yahoo.fr

* Contribution to the topical issue "Materials for Energy Harvesting, Conversion and Storage (ICOME 2015) - Elected submissions", edited by Jean-Michel Nunzi, Rachid Bennacer and Mohammed El Ganaoui

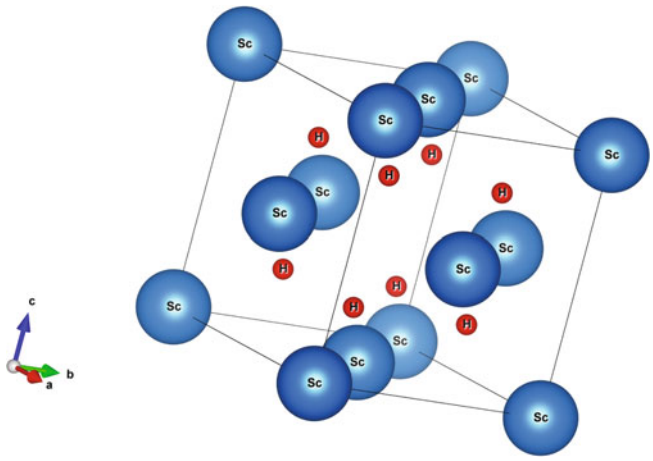

Fig. 1. Crystal structures of ScH_2.

Table 1. Relaxed lattice constants compared with experimental work.

	Our work		Experimental
	LDA	GGA	–
a (Å), ScH_2 (225, Fm-3m)	5.0041	4.9333	4.7796 [19]
Discrepancy (%)	4.70	3.21	–

Martins [17] and generalized gradient approximation (GGA) to approximate the exchange-correlation energy. We employed the pseudo-potentials and plane waves method implemented in the ABINIT code [18].

The electronic wave functions were expanded in plane waves up to a kinetic energy cutoff of 40 hartree. Integrals over the Brillouin zone were approximated by sums of $8 \times 8 \times 8$ mesh of special k-point.

3 Results and discussion

3.1 Crystal structure of ScH_2

The ideal cubic structure of ScH_2 compounds (space group 225, see Fig. 1) contains one formula with the following Wyckoff positions of the atoms: Sc 4a $(0, 0, 0)$ and H 8c $(1/4, 1/4, 1/4)$ [19]. After lattice constant relaxation, we reported the results in Table 1. Our calculated values are in good agreement with the experimental ones. The discrepancy is less than 4.70% and 3.21% for LDA and GGA respectively which is acceptable compared to the accuracy for DFT Calculations [20]. This is sufficient to allow the further study of electronic and optical properties. However, the GGA gives better result than LDA for lattice constant parameter.

In Table 2, we reported the bonding distances of each element that composes the ScH_2 compound.

3.2 Enthalpy of formation

We calculated the ScH_2 enthalpy of formation using the following reaction:

$$ScH_2 \rightarrow Sc + H_2$$

Table 2. Calculated bonding distance compared with experimental work.

ScH_2	Our work		Experimental
	LDA	GGA	–
Sc-H (Å)	2.1668	2.1361	2.0696 [19]

Table 3. Calculated formation enthalpy of ScH_2.

Elements	Total energy (eV)		Enthalpy of formation (kJ/mol)	
	LDA	GGA	LDA	GGA
Sc	−60.992	−49.271	–	–
H_2	−30.823	−31.402	–	–
ScH_2	−93.841	−82.715	−195.547	−196.984
Theoretical work			−200 [2], −195.60 [21,24]	
Experimental works			−204.11 [21], −201.60 [22,23]	

We subtracted the total energies of the pure elements Sc (in hexagonal structure, space group 194) and the hydrogen molecule from their hydride ScH_2.

Table 3 contains the computed total energy and formation enthalpy of ScH_2 compound, Sc element and hydrogen molecule using LDA and GGA approximations. Our calculated values are in good agreement with the experimental data [21,22] and [23]. Also, our results are compared to the calculation one of Alapati et al. [2] and Ye et al. [21,24] and we found a good agreement.

3.3 Electronic density of states

In this section we used the relaxed lattice constants reported in Table 1 to investigate the electronic structure of the rare hydride compound ScH_2.

The total densities of states calculated with LDA and GGA approximations are plotted in Figures 2 and 3.

The electronic structures reveal that ScH_2 is metallic because there is no gap energy which agrees qualitatively the DOS reported by Er et al. [25] (metallic behavior, hydrogen states dominated at low energy). The DOS reaches a value of 0.8691 and 0.8368 (states/eV/cell) at the Fermi level (−4.320 and −3.660 eV) for LDA and GGA approximations respectively.

We present in Figures 4 and 5 the partial densities of electronic states (PDOS) calculated with LDA and GGA approximations. The contribution of Sc is very small in valence band. But the main contribution of Sc-d appears in increasing order of energy. At the bottom of PDOS energy, we can see two peaks; which are mainly produced by the H-s states, this means that H-s states are more present in the valence band (VB) than in the conduction band (CB). Also, we can note hybridization between Sc-d and H-s states (between −7 and −8.5 eV) this can explain the great value of formation enthalpy (the hybridization makes difficult to break the bond between Sc and H).

3.4 Optical properties

The optical properties of matter can be described by means of the dielectric function $\varepsilon(\omega)$. The dielectric

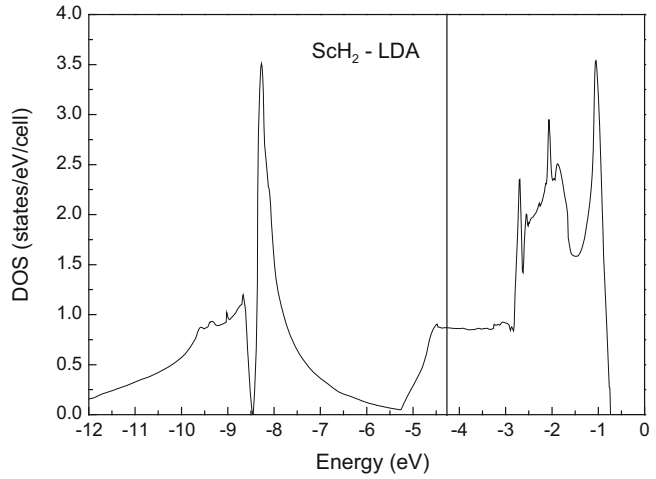

Fig. 2. The total density of state of ScH_2 calculated with LDA approximation. The vertical line presents the Fermi level.

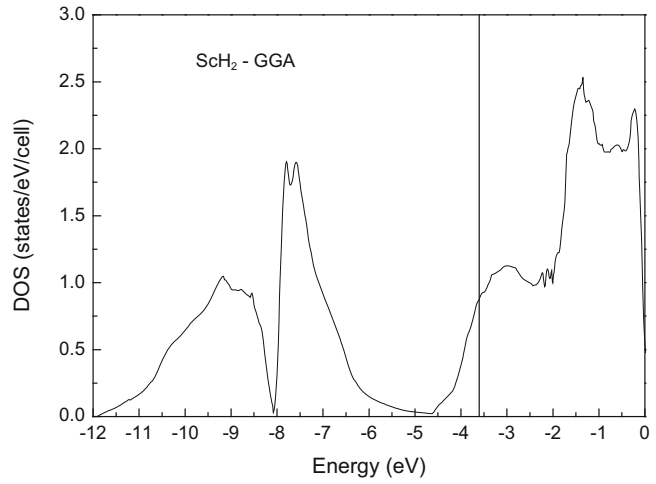

Fig. 3. The total density of state of ScH_2 calculated with GGA approximation. The vertical line presents the Fermi level.

function (only inter-band contribution) has the following form:

$$\varepsilon(\omega) = \varepsilon_1(\omega) + i\varepsilon_2(\omega). \quad (1)$$

In this study, the imaginary part of the dielectric function is calculated by summing transitions from occupied to unoccupied states over the BZ, weighted with the appropriate momentum matrix elements and given by [26,27]:

$$\varepsilon_2(\omega) = \frac{4\pi^2 e^2}{m^2\omega^2} \sum_{i,j} \int |\langle i\,|P|\,j\rangle|^2 (f_i(1-f_j)) \times \delta(E_f - E_i - \hbar\omega) d^3k, \quad (2)$$

where P is the momentum operator, and are the electron charge and mass, respectively. ω is the frequency of the photon and $|j\rangle$ are the eigenfunctions with eigenvalues E_i and E_j respectively. f_i and f_j are the Fermi distribution for $|i\rangle$ and $|j\rangle$ state respectively.

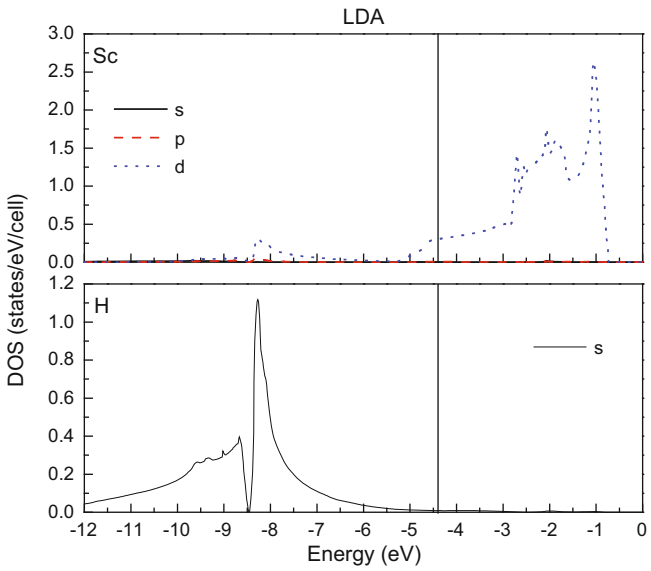

Fig. 4. The partial density of state of ScH_2 calculated with LDA approximation. The vertical line presents the Fermi level.

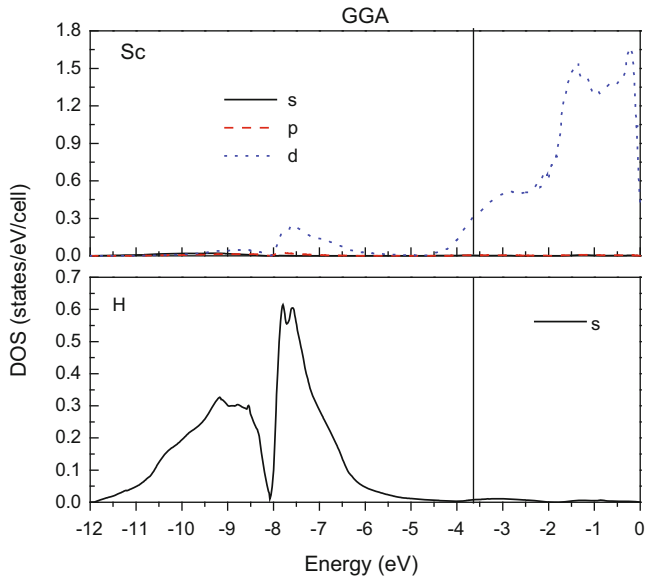

Fig. 5. The partial density of state of ScH_2 calculated with GGA approximation. The vertical line presents the Fermi level.

The real part of the dielectric function can be extracted from $\varepsilon_2(\omega)$ using the Kramers-Kronig relation:

$$\varepsilon_1(\omega) = 1 + \frac{2}{\pi} \int_0^\infty \frac{\varepsilon_2(\omega')\omega' d\omega'}{\omega'^2 - \omega^2}. \quad (3)$$

The knowledge of both the real and imaginary parts of the dielectric function $\varepsilon(\omega)$ allows the calculation of the important optical constants such as the refractive index $n(\omega)$, extinction coefficient $k(\omega)$, optical reflectivity $R(\omega)$, absorption coefficient $\alpha(\omega)$ and energy-loss spectrum $L(\omega)$ [28].

In Figure 6, the imaginary and the real part of the dielectric function is plotted as a function of photon energy for ScH_2.

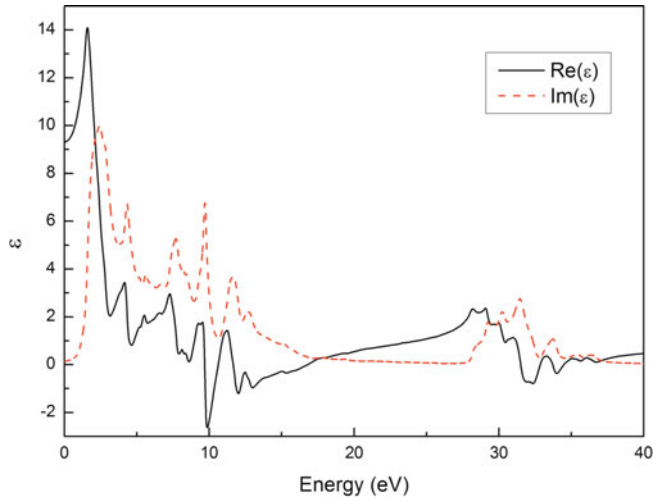

Fig. 6. The calculated real (Re(ε)) and imaginary (Im(ε)) parts of the dielectric function of ScH_2.

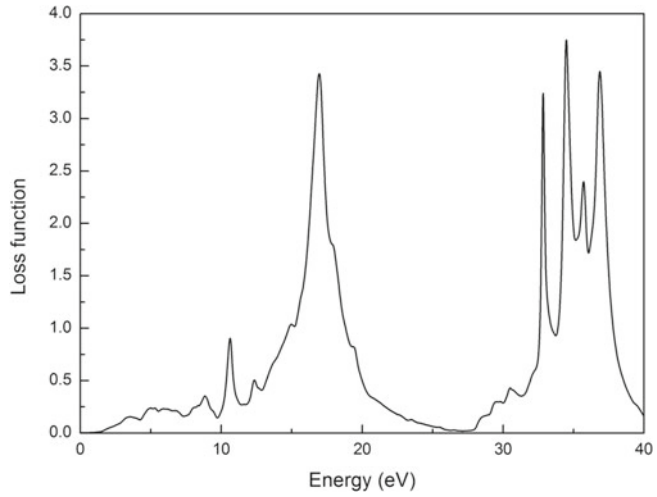

Fig. 7. Electron energy loss function $L(\omega)$ of ScH_2.

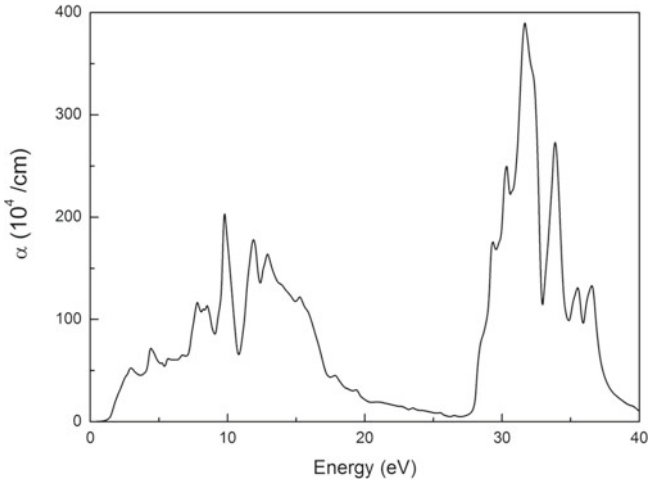

Fig. 8. Calculated absorption coefficient (α) of ScH_2.

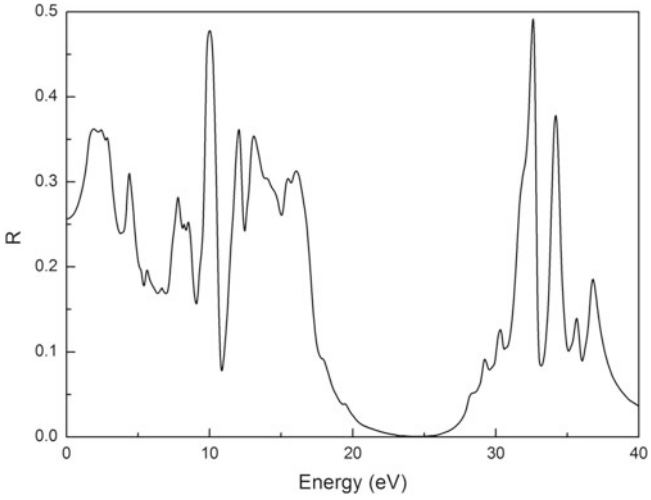

Fig. 9. Reflectivity spectrum of ScH_2.

Im($\varepsilon(\omega)$) has major peaks and minor peaks. The peaks in the optical response are caused by the electric-dipole transitions between the valence and conduction bands. It is noted that a peak in Im($\varepsilon(\omega)$) does not correspond to a single interband transition since many direct transitions may be found in the band structure with an energy corresponding to the same peak. The dielectric constant Re($\varepsilon(0)$) is given as 9.32 for ScH_2.

The calculated energy-loss function, $L(\omega)$ of ScH_2 is also presented in Figure 7. The function $L(\omega)$ describes the energy loss of fast electrons traversing the material. The sharp maxima in the energy-loss function are associated with the existence of plasma oscillations [29]. From Figure 2 we can see that there are four peaks at 15.6, 32, 35 and 36 eV.

The calculated absorption coefficient for ScH_2 is shown in Figure 8, from which we can see that there is no absorption in the high energy region $>$ 40 eV, implying that the electron is hard to respond when the wavelength of the incoming photons is shorter than 30.9 nm.

The calculated spectrum of the reflectivity coefficient $R(\omega)$ for ScH_2 is plotted in Figure 9. The reflectivity coefficient has a value of 26% or the zero frequency limits.

The $R(\omega)$ increases with the increasing photon energy to reach a maximum value of about 36% for photon energy of 1.9 eV, then it decreases to 17% for photon energy of about 6 eV and then it increase again to reach its second maximum of about 47% for photon energy of 10 eV, then it decreases to $\approx$0% at 24 eV and increases to reach its third maximum (37%) at 31 eV.

To show the effect of hydrogen on optical properties of scandium, we calculated in the same conditions, the optical reflectivity of Sc and we drew it in Figure 10. In the visible light range (1–3 eV), the reflectivity of ScH_2 is smaller than that of Sc but not enough to be transparent which is expected for dihydride rare-earth [1]. This is can be explained by the absence of metal to semiconductor transition from Sc(metal) to ScH_2(metal). However,

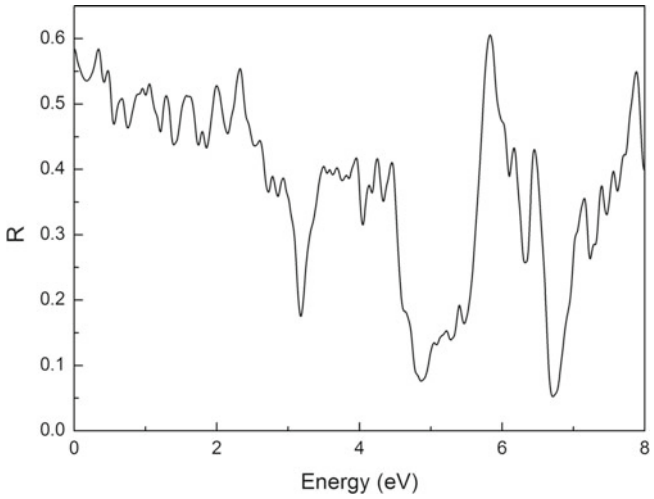

Fig. 10. Reflectivity spectrum of Sc.

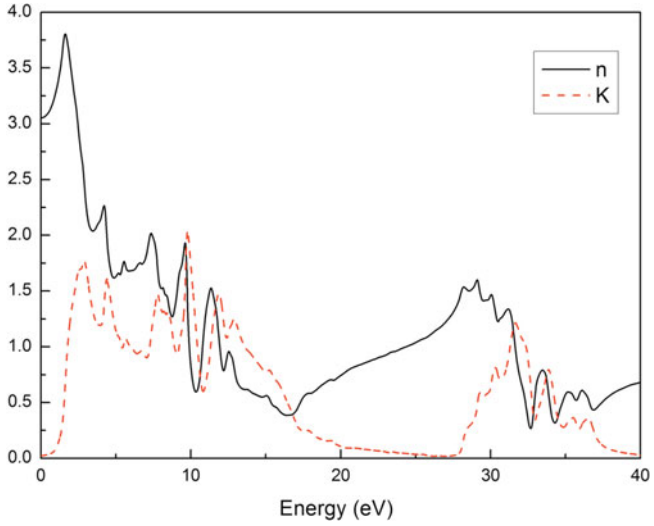

Fig. 11. Refractive index $n(\omega)$ and extinction coefficient $k(\omega)$ of ScH_2.

ScH_3 under high pressure is semiconductor [30], which the existence of metal to semiconductor transition in ScH_x $(2 < x < 3)$ (switchable metal-insulator material [1]).

The refractive index $n(\omega)$ and the extinction coefficient $k(\omega)$ are displayed in Figure 11. The refractive index spectrum indicates that the static refractive index $n(0)$ has a value of 3.05.

4 Conclusion

First principal calculations for ScH_2 compound was performed in this study using the pseudo-potentials and plane wave method implemented in the DFT. The enthalpy of formation for this rare-earth hydride is calculated for two different approximations (LDA and GGA) and they are in good agreement with theoretical work. This allowed us to better analyze our compound by studying the DOS and PDOS. Also from the plot of these electronic densities of states, we noted that ScH_2 has no gap which means that our compound is a metallic and the valence band is dominated by hydrogen atoms. Finally, we can note hybridization between Sc-*d* and H-*s* states which can explain the high value of formation enthalpy.

The optical properties are presented in this study, and they have been described by means of the dielectric function $\varepsilon(\omega)$.

References

1. R. Griessen, I.A.M.E. Giebels, B. Dam, *Hydrogen as a Future Energy Carrier*, edited by A. Züttel, A. Borgschulte, L. Schlapbach (Wiley-VCH Verlag GmbH & Co. KGaA, Weinheim, Germany, 2007), p. 326
2. S.V. Alapati, K.J. Johnson, D.S. Sholl, Phys. Chem. Chem. Phys. **9**, 1438 (2007)
3. A.G. Aleksanyan, S.K. Dolukhanyan, V.Sh. Shekhtman, Kh.S. Harutyunyan, K.A. Abrahamyan, N.L. Mnatsakanyan, J. Alloys Compd. **356–357**, 562 (2003)
4. S.K. Dolukhanyan, H.G. Hakobian, A.G. Alexanian, Int. J. SHS **1**, 530 (1992)
5. S.K. Dolukhanyan, J. Alloys Compd. **253–254**, 10 (1997)
6. G. Sandrock, G. Thomas, Appl. Phys. A **72**, 153 (2001)
7. P.H. Smith, K.H.J. Buschow, Phys. Rev. B **21**, 3839 (1980)
8. G.S. Burkhanov, N.B. Kol'chugina, O.D. Chistyakov, V.N. Verbetsky, A.A. Salamova, E.Yu. Andreeva, E.S. Volkova, Inorg. Mater. **42**, 491 (2006)
9. X. Luo, D.M. Grant, G.S. Walker, J. Alloys Compd. **622**, 842 (2015)
10. P.H.L. Notten, M. Ouwerkerk, H. van Hal, D. Beelen, W. Keur, J. Zhou, H. Feil, J. Power Sourc. **129**, 45 (2004)
11. J.H. Weaver, R. Rose, D.T. Peterson, Solid State Commun. **25**, 201 (1978)
12. J.H. Weaver, R. Rose, D.T. Peterson, Phys. Rev. B **19**, 4855 (1979)
13. R. Griessen, J.N. Huiberts, M. Kremers, A.T.M. van Gogh, N.J. Koeman, J.P. Dekker, P.H.L. Notten, J. Alloys Compd. **253–254**, 44 (1997)
14. I.O. Bashkin, E.G. Ponyatovskii, M.E. Kost, Phys. Status Solidi B **87**, 369 (1978)
15. T.C. Messina, C.W. Miller, J.T. Markert, Phys. Rev. B **75**, 104109 (2007)
16. W. Kohn, L.J. Sham, Phys. Rev. **140**, A1133 (1965)
17. N. Troullier, J.L. Martins, Phys. Rev. B **43**, 1993 (1991)
18. X. Gonze, J.M. Beuken, R. Caracas, F. Detraux, M. Fuchs, G.-M. Rignanese, L. Sindic, M. Verstraete, G. Zerah, F. Jollet, M. Torrent, A. Roy, M. Mikami, Ph. Gohsez, J.Y. Raty, D.C. Allan, Comput. Mater. Sci. **25**, 478 (2002)
19. M. Latroche, W.P. Kalisvaart, P.H.L. Notten, J. Solid State Chem. **179**, 3024 (2006)
20. D.S. Sholl, J.A. Steckel, *Density Functional Theory: A Practical Introduction* (John Wiley & Sons, Inc. New Jersey, USA, 2009), p. 252
21. X. Ye, T. Tang, B. Ao, D. Luo, G. Sang, H. Zhu, J. Fusion Energ. **32**, 254 (2013)
22. F.D. Manchester, J.M. Pitre, J. Phase Equilib. **18**, 194 (1997)

23. M.L. Lieberman, P.G. Wahlbeck, J. Phys. Chem. **69**, 3514 (1965)
24. X. Ye, R. Hoffmann, N.W. Ashcroft, J. Phys. Chem. C **119**, 5614 (2015)
25. S. Er, D. Tiwari, G.A. de Wijs, G. Brocks, Phys. Rev. B **79**, 024105 (2009)
26. C. Ambrosch-Draxl, J.O. Sofo, Comput. Phys. Commun. **175**, 1 (2006)
27. Y. Bouhadda, Y. Boudouma, N. Fenineche, A. Bentabet, J. Phys. Chem. Solids **71**, 1264 (2010)
28. F. Wooten, *Optical Properties of Solids* (Academic Press Inc., New York, USA, 1972), p. 272
29. L. Marton, Rev. Mod. Phys. **28**, 172 (1972)
30. T. Pakornchote, T. Bovornratanaraks, S. Vannarat, U. Pinsook, Solid State Commun. **225**, 48 (2016)